DOI:10.28974/idojaras.2025.1.1

IDŐJÁRÁS

Quarterly Journal of the HungaroMet Hungarian Meteorological Service
Vol. 129, No. 1, January – March, 2025, pp.1–14

Comparison of horizontal visibility observed by present weather sensor and human eye-based method and evaluated from ceilometer's vertical backscattering profile over two Hungarian meteorological stations

András Peterka*, **Gabriella Schmeller**, **Noémi Sarkadi**, and **István Geresdi**

Institute of Geography and Earth Sciences
Faculty of Sciences
University of Pécs
Ifjúság útja 6., H-7624 Pécs, Hungary

* *Correspondening Author E-mail*: *peterka.andras@gmail.com*

(Manuscript received in final form February 1, 2024)

Abstract— This research aims to evaluate a quantitative comparison of the visibilities detected by three different methods: (i) human eye-based observations; (ii) calculated from the measured values of forward scatter visibility sensor; and (iii) evaluated from ceilometer's vertical backscattering profiles. Visibility data observed at two meteorological stations, Pestszentlőrinc and Szeged (Hungary) were analyzed. The paper focuses on the fog events observed during the periods of October-December in 2019 and November 21-24 in 2020. The results reveal that the visibility observed by the three methods can be significantly different. Comparison of the values of visibility detected by the three different techniques shows, that visibility evaluated from the ceilometer data is the largest, and the human eye-based observation detects the smallest values. Analysis of the data about fog detection (yes or no) reveals that the ceilometer detects significantly shorter duration of the fog than the other two methods.

Key-words: visibility, ceilometer, fog, present weather sensor, human-eye based observation

1. Introduction

Visibility has a direct and indirect effect on our everyday life. It significantly influences the safety of transport (road traffic, aviation, shipping, etc.) (*Wang et al*., 2017; *Shepard,* 1996) and human health (*Hameed et al*., 2000) as well. Visibility is impacted by meteorological parameters, e.g., relative humidity, temperature, and wind speed (*Zhao et al*., 2013). Thus, through measurement of visibility, conclusions may be derived for the atmospheric circumstances.

Visibility is usually observed by human-eye observation or sensors that are based on different optical principles, e.g., light transmission, and forward scattering (transmissometers and forward scatter sensors) (*Chan*, 2016). Because visibility depends on the backscattering of light, it can be determined by a ceilometer (*Taillade et al*., 2008; *Czarnecki et al*., 2014).

Kim (2018) compared the visibility values detected by human eye-based, image-based, and optical-based methods. While the human eye-based and optical-based measurements were performed at the Seoul Meteorological Observatory, the image-based measurements occurred about 3 km northwest of the observatory. The author asserted that the calculated image-based visual range agreed better with the human eye-based visual range than that detected by the optical-based meteorological optical range (hereafter MOR) sensor. *Cheng et al*. (2018) emphasized that the worldwide used optical measurement techniques had several limitations, thus alternative methods for determining atmospheric visibility are needed. The authors implemented a novel algorithm to test the accuracy of visibility data measured by a vision-based method (video surveillance cameras). They concluded that the "variation approach provides an effective and efficient framework for real-time atmospheric visibility estimation" (*Cheng et al*., 2018). *Wang et al*. (2014) suggested a new Digital Photography Visiometer System (DPVS) for automatic visibility determination which operates in the same way as the human eye-based method (hereafter HEM) and could replace them in any kind of weather conditions. They compared the data detected by DPVS with a forward scattering visibility instrument (FD12), and manual observations in heavy rainfall, even- and uneven rainfall, non-rainy and foggy conditions. They concluded that during heavy rainfall events, visibility is negatively correlated to the intensity of the precipitation. During even- and uneven rainfall events, the visibility values detected by manual observation and DPVS agreed well. However, the visibility detected by the forward scatter meter was smaller, and the variability of its values was significantly larger. In the case of non-rainy (or clear) conditions, the visibility values detected by each of the three methods agreed well. In foggy conditions, the bias between the values was small. They found that comparing values detected by the forward scatter meter and DPVS to that observed by the HEM during e.g., rainy conditions, the DPVS gives more accurate visibility values, while the forward scatter meter seems to be less accurate.

As ceilometers can be operated during any kind of weather conditions and both daytime and nighttime, these devices give continuous information about the vertical profile of the atmosphere. Based on these properties, ceilometers can be efficiently used as tools for automated mixing height measurements, for the estimation of in situ PM_{10} concentrations (*Münkel et al*., 2006), surface $PM_{2.5}$ concentrations even during cloudy and nighttime conditions (*Li et al*., 2017), and also for the monitoring of diurnal, seasonal, and vertical changes of aerosol layers (*Muñoz et al*., 2012). Furthermore, ceilometers have been implemented in the fog alert systems (*Haeffelin et al*., 2016) and in skyglow simulations (*Kolláth et al*., 2020).

Continuously working ceilometer CHM15k systems are already deployed over 11 places in Hungary. Integrating them to the current visibility measuring systems does not require further investment, and it would spatially improve the availability of visibility data. Utilizing them to evaluate visibility would fit in the global trend to rely more on automated systems over human observers.

Molnar et al. (2008) elaborated the spatial distribution of visibility observed in 1996 and 2002 in Hungary. They found that the annual average visibility was 4 km larger in 2002 than in 1996. The regional variability is ambiguous: while in the northern and western parts of the country the increase of visibility was larger than the average, in the central region (mainly the Great Hungarian Plain) the increase of the visibility was smaller This difference stems from that fact that while in the northern and western parts of the country the visibility reduction is the consequence of the industrial emission, in the Great Hungarian Plain the dust particles emitted from the sandy soil reduces the visibility. The reduction of the industrial emission at the end of the last century must have resulted in significant increase of the visibility.

In this study, horizontal visibility was calculated from ceilometer data based on the Koschmieder formula and the Klett-Fernald algorithm. This visibility data was compared with that observed by the human eye and present weather-visibility sensors. Data observed during 39 foggy events (when the visibility detected by any of the methods is less than 1000 m) occurred at two locations were analyzed to characterize the differences between the three methodologies. Furthermore, 2 cases were chosen to make a more detailed analysis. Section 2 describes the visibility measurement methods, the calculation from ceilometer data, and the selected cases. Section 3 presents the results, and summary of the paper is given in Section 4.

2. Data and methods

The Hungarian Meteorological Service (hereafter HungaroMet) operates the national meteorological measurement network. In this network, regular human eye-based visibility observations are carried out at 14 meteorological stations and

3 air force bases. Trained observers estimate the horizontal visibility values based on the regulations of the WMO (WMO, 2021). The observation methods in these stations are either human eye-based or remote sensing including the data of forward scatter meters, disdrometers, and/or sky cameras installed at the stations.

Few stations (including the Marczell György Main Observatory in Budapest and the Upper Air Observatory in Szeged) are equipped with the PWD22 (Vaisala, Finland) Present Weather Detector and Visibility Sensor (henceforth: PWVS) which is designed to observe the horizontal visibility within a range from 10 to 20,000 meters. The device operates by the right of the forward scatter principle. Both the emitter and receiver units are tilted down at a 45° angle. The scattering of emitted light depends on its wavelength and the size of the drops. The intensity of the forward scattered light is proportional to the number concentration of the particles. Because the droplet size in the fog is significantly smaller than the size of the precipitating hydrometeors, this instrument can distinguish the fog from the falling precipitation (and even more types of precipitation can be determined, such as snow or freezing rain). Besides visibility and precipitation type, the intensity of precipitation is also measured.

CHM15k Nimbus ceilometers (Lufft, Germany) are installed at four meteorological stations in the Hungaromet network: Marczell György Main Observatory in Pestszentlőrinc, Upper Air Observatory in Szeged, Storm Warning Observatory in Siófok, and the meteorological station at the University of Pécs. The wavelength of the radiation emitted by the CHM15k Nimbus ceilometers is 1.064 μm (User Manual CHM 15k.).

In this study visibility values retrieved by three different methods are compared: 1) human eye-based observations, 2) visibility values from forward scatter visibility sensor (PWVS), and 3) visibility values calculated from the backscatter profile of ceilometer measurements. To the authors' knowledge, the observers can utilize data from sky cameras or PWVS in the HEM. Therefore, HEM and PWVS may not be independent.

Due to the low number of ceilometers in the network, visibility data observed at two Hungarian meteorological stations (Pestszentlőrinc and Szeged) were selected for comparison. At these two stations, the selected optical-based sensors and regular human eye-based visibility observations are available.

The vertical profile of the backscattered energy assessed by a ceilometer was used to evaluate the visibility. The evaluation of visibility based on the Koschmieder formula (*Larson* and *Cass*, 1989):

$$VIS = \frac{-ln0.02}{\sigma_{ext}}, \qquad (1)$$

where σ_{ext} is the extinction coefficient. The vertical profile of the extinction coefficient and the mean extinction coefficient of the column at a given time were evaluated by the Klett-Fernald algorithm (*Werner et al.*, 2006; 28902-1:2012 ISO standard) implemented in MATLAB R2020b. For this evaluation, the following conditions were set:

1. Due to the attenuation of the beam, ceilometers cannot detect the upper part of the fog (*Nowak et al*., 2008). Therefore, negative backscatter values can appear. These values cannot be incorporated into the calculations, thus they are treated as NaN.
2. If the sky condition index of the ceilometer indicates fog, but the column contains less than 10 non-NaN values due to the attenuation of the beam, that indicates a rather dense fog. In those cases the mean of the extinction coefficient for the column is set to 0.03

We hypothesize that the fog is isotropic in the surroundings of the ceilometer, thus the backscattered energy detected vertically (calculated from the backscatter profile) equals to the horizontal one (note that data near to the surface in the so-called blind range are not available, this may also cause error in visibility detection). Please note that while the condition of the isotropic surroundings is often met, currently we cannot distinguish those cases where it fails. If the surrounding area was not isotropic, the evaluated visibility would not be correct.

Fog events detected in October-December 2019 and November 2020 were selected for comparison. Data observed on total of 20 days at Budapest (Marczell György Main Observatory in Pestszentlőrinc), and at Szeged (Upper Air Observatory) were analyzed. Furthermore, a well-observed radiation fog event on November 24, 2020 (*Gandhi et al*., 2023) was chosen for a case study (*Table* 1).

Table 1. Days selected for data evaluation. The data observed on the day highlighted with bold letters are chosen for case study.

	Pestszentlőrinc	**Szeged**
October 2019	-	10 / 26
November 2019	04 / 05 / 07 / 08 / 09 / 27 / 28 / 29	04/ 05 / 08 / 09 / 15 / 25 / 29
December 2019	04 / 05 / 07 / 08 / 09 / 12 / 13 / 16 / 19 /21	03 / 05 / 06 / 07 / 08 / 09 / 10
November 2020	23 / **24**	21 / 22 / 23 / **24**
Total	20	20

The visibility values evaluated from the ceilometer backscattering profile and the PWVS visibility data have a 1-minute temporal resolution. However, the frequency of human eye-based observations is only 1 hour. For the comparison of the data, 15-minute averages were created from the 1-minute data set, and the 1-hour dataset was divided into sections with a duration of 15 minutes. That means there are 1920 elements of the dataset observed at Budapest station, and there are 1920 elements of the dataset observed at Szeged station.

The difference between the visibility values derived from different methods is quantified by plotting histograms and by evaluation of contingency tables. The histograms reveal the frequency of the relative difference *x* between the visibilities evaluated by the two different methods:

$$x = \frac{h1-h2}{(h1+h2)/2}, \quad (2)$$

where $h1$ and $h2$ are the visibilities evaluated by method 1 and method 2, respectively. The histogram was normalized, the height of a bar was calculated by the following formula:

$$y = \frac{n}{w*N}, \quad (3)$$

were *n* is the count of the bin, *w* is the width of the bin, and *N* is the total count. The bin's width of the histogram is 0.25. The data for the evaluation of the histogram were involved if any of the two methods detected fog. The differences are plotted for the following pairs of methods: (a) PWVS – Ceilometer, (b) PWVS - HEM, and (c) HEM - Ceilometer.

The reliability of simple fog detection (yes or no) is also an important characteristic of the fog detection methods. For the comparison of the fog detection, contingency tables were prepared using visibility data evaluated for intervals of 15 minutes. Based on the contingency table, the frequencies of fog detection by the different methods are compared. The critical success index (hereafter *CSI*) and *bias* were evaluated:

$$CSI = a/(a + b + c), \quad (4)$$

$$bias = (a+b)/(a+c), \quad (5)$$

where *a* is the number of hits (top left corner of the contingency table), *b* is the number of misses (top right corner of the contingency table), and *c* is the number of false alarms (bottom left corner of the contingency table).

3. Results and discussion

3.1. Comparison of PWVS and ceilometer

Histograms in *Fig.1* reveal the differences between the visibilities detected by different methods. The frequency of the relative differences (see Eq.(2)) for the comparison of the PWVS and ceilometer at the Budapest and Szeged stations are plotted in the first row in panels (a1) and (a2), respectively. In the case of Budapest (pane1 a1), the relative differences of the measured visibility vary between -0.50 and 1.25 and show a right-skewed pattern. That means that in most of the cases (the total number of cases, when any of the two methods detected fog, is 358), the visibility evaluated from ceilometer data is significantly larger than that of observed by PWVS (274 from 358), and the visibility observed by PWVS is larger only about in one-third of the cases (83 from 358). The highest frequency of the relative difference for the visibility is between -1.25 and -0.50. However, there is a significantly smaller second mode, at about a relative difference of 0.75. The standard deviation (hereafter STD) of the dataset is 0.67. Data from Szeged (panel a2) show a similarly right-skewed pattern. However, the distribution is wider, indicated by a larger STD of 0.84 (panel a2). The relative difference of visibility varies between -2.00 and 1.50, and a large relative difference can be observed in a wider range, between -1.75 and -0.50. Similarly, to the Budapest data, there is a significantly smaller second mode at the positive values of the relative difference, at around 1.25.

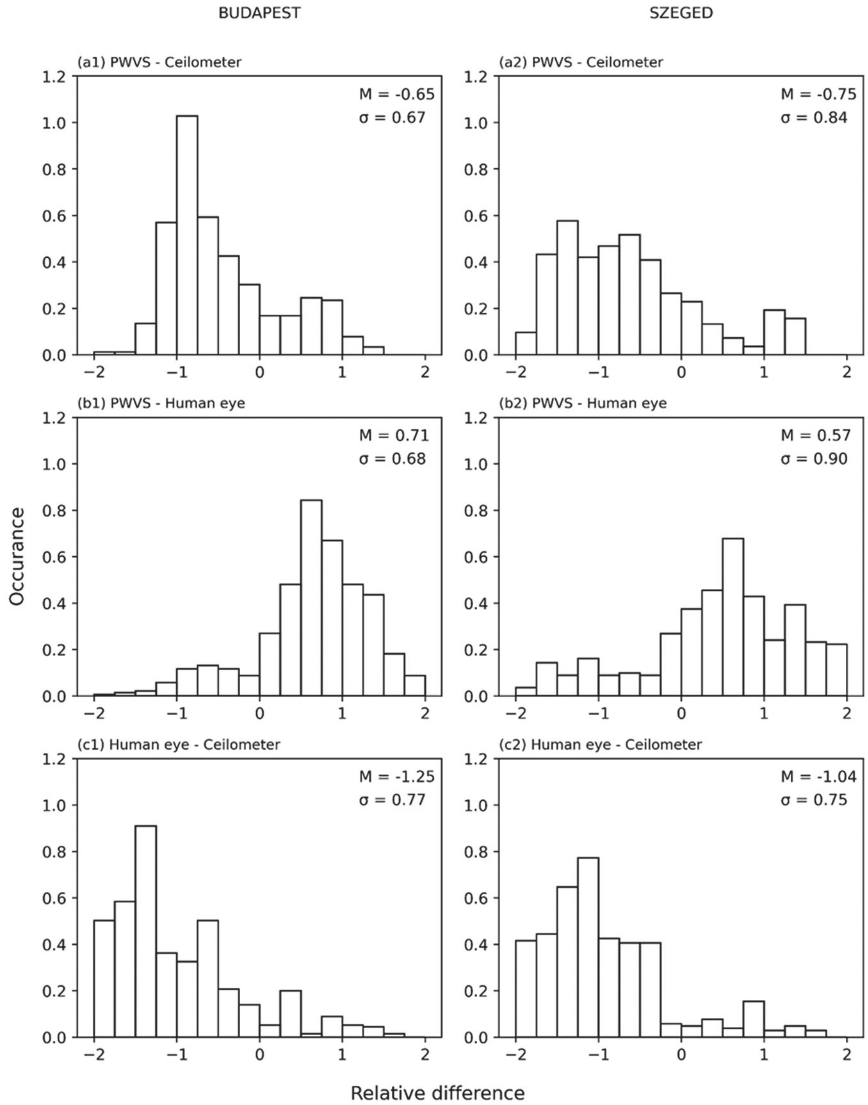

Fig. 1. Relative differences in the 15-minute average visibility values during fog on histograms in Budapest (1) and Szeged (2). (a) differences between PWVS and ceilometer, (b) differences between PWVS and HEM, and (c) differences between HEM and ceilometer. M is the median and σ is the standard deviation.

Fig.2 also shows that both in Budapest (panel a) and Szeged (panel b) there is only a limited number of cases when the ceilometer detected fog, while PWVS did not. The scatter plots in *Fig.2* allow us to conclude that there is no correlation between the visibility values evaluated by the two different methods. Scatter plots were created for the other two method pairs, however, valuable information cannot be derived from them.

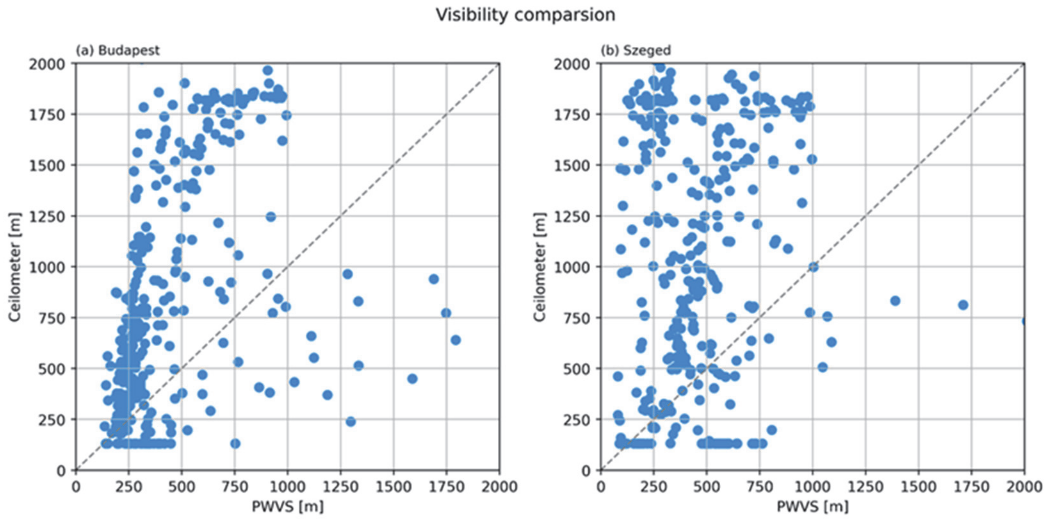

Fig. 2. Relation between visibilities, evaluated from PWVS (x-axis) and ceilometer (y-axis) data at Budapest (panel a) and Szeged (panel b). Gray dashed lines denote the one-to-one relation.

3.2. Comparison of PWVS and HEM

Fig.1 panels b1 and b2 show the comparison of the visibilities detected by PWVS and HEM in Budapest and Szeged, respectively. In Budapest, the data shows a single modal left-skewed distribution, where the relative differences vary between -1.25 and 2.00. The highest value of the peak is between 0.50 and 0.75, while most of the data points spawn between 0 and 1.50. A significantly smaller mode is around -0.75 – -0.50, which is the consequence of a limited number of cases (35) when the PWVS detected fog, while the HEM did not (*Table 2,* panel b). In Szeged data, there is a single modal left-skewed distribution. Compared to Budapest, the single peak is smaller, but it can be found in the same bin between 0.50 and 0.75. The range where most of the data points can be found is wider spawning between -0.25 and 2.00. The wider distribution is also shown by the larger STD (0.90 compared to 0.68). Panel b of *Table 2* shows that the number of cases when HEM detected visibility and PWVS did not is higher than vice versa. However, the difference is less compared to the PWVS-ceilometer comparison. Both the Szeged and Budapest datasets show that the visibility values observed by HEM is significantly smaller than the visibility detected by PWVS.

Table 2. Contingency tables comparing the different methods based on whether fog was detected or not in Budapest (first value) and Szeged (second value). (a) PWVS and ceilometer, (b) PWVS and HEM, and (c) HEM, and ceilometer.

(a) PWVS \ Ceilo	**Detected**	**Not detected**	**Total**
Detected	224 | 161	120 | 168	344 | 329
Not Detected	14 | 4	1562 | 1587	1576 | 1591
Total	238 | 165	1682 | 1755	1920 | 1920

(b) PWVS \ HEM	**Detected**	**Not detected**	**Total**
Detected	309 | 281	35 | 48	344 | 329
Not Detected	111 | 87	1465 | 1504	1576 | 1591
Total	420 | 368	1500 | 155	1920 | 1920

(c) HEM \ Ceilo.	**Detected**	**Not detected**	**Total**
Detected	220 | 151	200 | 217	420 | 368
Not Detected	18 | 14	1482 | 1538	1500 | 1552
Total	238 | 165	1682 | 1755	1920 | 1920

3.3. Comparison of HEM and ceilometer

Panels c of *Fig.1* show the differences in visibility between HEM and ceilometer in Budapest and Szeged. The data from Budapest show a single modal right-skewed distribution, where the highest frequency is between -1.25 and -1.50, while most of the data can be found in the range of -2.00 – 0.50. From the peak to the end of the tail of the distribution, the height of the bins is gradually decreasing, compared to Szeged, where the transition from the peak to the tail is rather sudden. The highest frequency in the Szeged dataset is between -1.50 and -1.00, while most of the values spawn in the range of -2.00 – -0.25. The sudden decrease in the transition from the peak to the tail occurs at -0.25, where the frequency drops from 0.4 to less than 0.1. The STD of the data sets are also similar (0.77 and 0.75). Panel c of *Table2* shows that HEM detected more cases than ceilometer at those times when just one of the methods detected fog. To conclude, the visibility values observed by HEM were lower than those by the ceilometer.

A 2×2 contingency table (*Table 2*) were prepared to evaluate skill scores for the fog detection. In this analysis, only the data about the fog detection (yes or no) are compared. PWVS detected 344 and 329 foggy time intervals in Budapest and

Szeged, respectively. HEM detected 420 and 368 foggy time intervals in Budapest and Szeged, respectively. Ceilometer detected 238 and 165 foggy time intervals in Budapest and Szeged, respectively. This means that fog was detected for the longest duration by HEM followed by PWVS and ceilometer at both stations. Accordingly, the method pair with the highest number of cases, where both methods detected fog is the PWVS - HEM (309 / 281), followed by the PWVS - ceilometer (224 / 161), and lastly the HEM - ceilometer (220 / 151). *Table 3* shows accuracy attributes of the contingency tables. The trend of the CSI values also follows the previous order The largest is the PWVS – HEM (0.68 / 0.68), followed by the PWVS - ceilometer (0.63 | 0.48), and the smallest is the HEM – ceilometer (0.50 / 0.40). To conclude, during fog, the observed visibility values differ for the three methods. Calculated visibility from the ceilometer is usually higher than that of from PWVS and HEM, and visibility observed by HEM is usually the lowest. In most cases, the trend of the difference (whether the difference is negative or positive) between the two methods is well defined. This can be also shown by the bias. values (*Table 3*), where the weakest is the PWVS – HEM (0.82 | 0.89). However, the exact reason of the difference is unknown.

Table 3. CSI and bias of the three compared method pairs.

Budapest | Szeged	**PWVS – Ceilo.**	**PWVS - HEM**	**HEM - Ceilo**
CSI	0.63 | 0.48	0.68 | 0.68	0.50 | 0.40
bias	1.45 | 1.99	0.82 | 0.89	1.76 | 2.23

3.4. Case study

On November 24, 2020, a radiation fog formed throughout the Carpathian Basin in the early hours and lasted even until late night in some regions of the country.

Fig.3 shows the time evolution of the visibility detected by the 3 different methods in Budapest (panel a) and Szeged (panel b). In Budapest, the fog formation was detected at 03:00 UTC by all the three methods. However, in the case of the ceilometer, the visibility starts to rise at ~14:00 UTC and reaches 1000 m by 15:00 UTC. Until 19:00 UTC it remains close to 1000 m, and after this time it indicates the dissipation of the fog due to the rising of the visibility to 2000 m. The other two methods detected fog dissipation later, at about 22:00 UTC. However, each of the three methods detected fog between 03:00 UTC and 19:00 UTC, the discrepancy for the fog detection occurs in a shorter time interval of 3 hours. Note, that shortly after the fog formed (after 06:00 UTC), when the visibility must have been the smallest, the ceilometer and HEM data agree well. Both methods detected visibility as small as 100 m between 08:00 and 09:00 UTC. Later the visibility detected by the PWVS and HEM agree well, and the values evaluated from ceilometer data may overestimate the visibility. In the dissipation phase (14:00 UTC–21:00 UTC) the largest difference between the visibility detected by the ceilometer and HEM has a maximum value of 900 m at ~17:50 UTC. However, the trends of visibility evaluated by the three methods are similar. The sudden and significant rise of the visibility in the case of the ceilometer may indicate that using this method for visibility detection is not reasonable in cloudy or clear sky conditions.

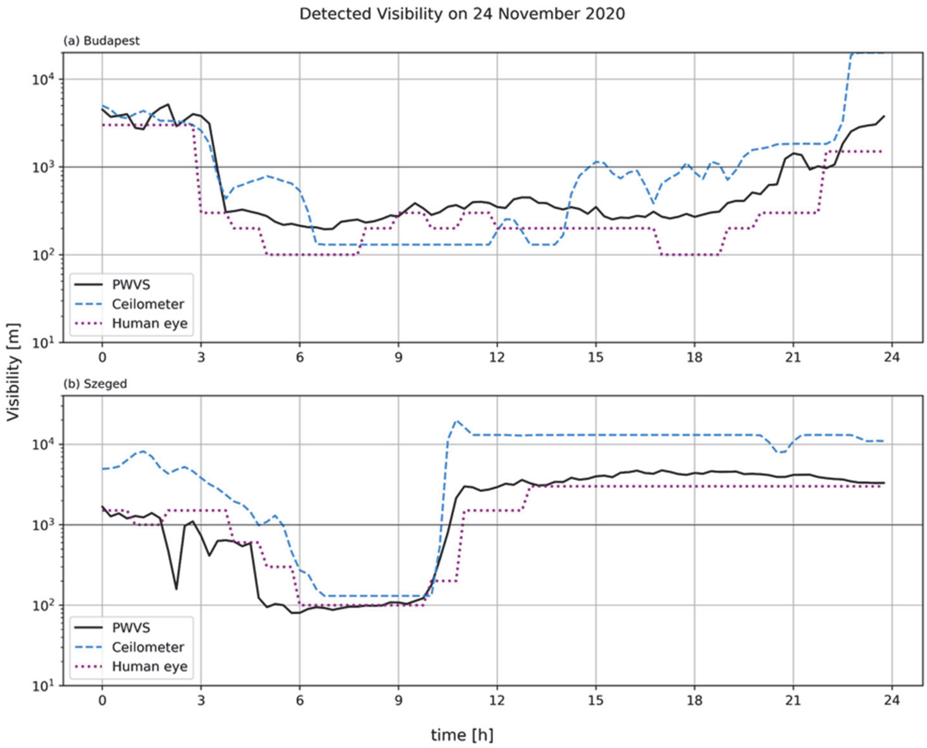

Fig. 3. Time evolution of visibility measured by PWS (solid black line), ceilometer (dashed blue line), and HEM (dotted purple line) in Budapest (a) and Szeged (b).

In Szeged (panel b), the three methods do not agree well in the time period of fog formation, which occurs between 02:00 UTC and 05:00 UTC, while values detected by HEM and PWVS are relatively close to each other during this period. The visibility evaluated from ceilometer data is significantly larger, it decreases from 5000 - 6000 m to 1000 m by 2–3 hours later than the other two methods. However, the coincidence is better in the dissipation period, which occurred at around 10:00 UTC. During the fog (06:00 UTC–10:00 UTC), the visibility evaluated by three methods agree well. Both the ceilometer and the two other methods detect dense fog with visibility of about 150 m and about 100 m, respectively. After the dissipation phase, the visibility values from PWVS and HEM are close to each other, compared to that of from ceilometer, as the later is constantly between 10,000–20,000 m, while the first varies between 3000–4000 m. This also indicates, that using of the ceilometer for the visibility evaluation is reasonable only in foggy weather and it is not reasonable in the case of the elevated fog or any other cloudy conditions.

4. Conclusion

In this research, horizontal visibility was evaluated from the vertical backscattering profile of the ceilometer, calculated with the Koschmieder formula and the Klett-Fernald algorithm. Visibility values evaluated from the ceilometer data were quantitatively compared to visibility data observed by PWVS and HEM.

Statistical analysis of the visibility data detected during foggy events in Budapest and Szeged station reveals: (i) Considering the fog detection (yes or no), best agreement was found between the PWVS and HEM methods (the CSI index is about 0.67). The largest discrepancy was found between the HEM and ceilometer method (the CSI index is about 0.50). That is these two methods give different results for the occurrence of the fog in about 50% of the data. (ii) Visibility values evaluated by the three variant methods can be significantly different. Statistical analysis of the relative differences reveals that the ceilometer gives the highest visibility values, followed by PWVS and HEM. (iii) The statistical analysis of the relative difference for the visibility and that of the contingency table for the fog detection disclose that the remote sensing technique of PWVS gives a better coincidence with the HEM than the ceilometer does. (iv) The results of the case study suggest that the three methods evaluate similar visibility in dense fog events, and even though the visibility values are different, the temporal trends are similar.

The authors hypothesize that the discrepancy between the different methods is the consequence of the different detection techniques. In the case of the ceilometer, it is supposed that the fog is homogeneous around the sensor. If the structure of the fog is not the same in horizontal and vertical directions, the visibilities that characterize the two directions can be different. While the sampling volume is a few m^3 in the case of the ceilometer, the PWVS has a rather small detection volume (few cm^3) which can result in differences between the two methods if the fog is inhomogeneous (e.g., large variability in the droplet concentration and/or droplet size).

Acknowledgements: This research was supported by GINOP-2.3.2-15-2016-00055 financed by the Ministry of Finance.

References

Chan, P.W., 2016: A test of visibility sensors at Hong Kong International Airport. *Weather 71,* 241–246. https://doi.org/10.1002/wea.2772

Cheng, X., Yang, B., Liu, G., Olofsson, T., and *Li, H.*, 2018: A variational approach to atmospheric visibility estimation in the weather of fog and haze. *Sust. Cities Soc. 39*, 215–224. https://doi.org/10.1016/j.scs.2018.02.001

Czarnecki, T., Perlicki, K., and *Wilczewski, G.*, 2014: Atmospheric visibility sensor based on backscattering using correlation coding method. *Opt. Quantum Electr. 47*, 771–778. https://doi.org/10.1007/s11082-014-9951-x

Gandhi et al, 2023: Fog Experiment in Budapest (2020–21). Micrometeorological measurements during foggy situations (submitted into Pure and Applied Geophysics)

Haeffelin, M., Laffineur, Q., Bravo-Aranda, J-A., Drouin, M.A., Casquero-Vera, J.-A., Dupont, J.-C., and *De Backer, H.*, 2016: Radiation fog formation alerts using attenuated backscatter power from automatic lidars and ceilometers. *Atmos. Measur. Tech. 9*, 5347–5365. https://doi.org/10.5194/amt-9-5347-2016

Hameed, S., Mirza, M.I., Ghauri, B.M., Siddiqui, Z.R., Javed, R., Khan, A.R., Rattigan, O.V., Qureshi, S., and *Husain, L.*, 2000: On the widespread winter fog in northeastern Pakistan and India. *Geophysical Research Letters*, *27*, 1891–1894. https://doi.org/10.1029/1999gl011020

Kim, K.W., 2018: The comparison of visibility measurement between image-based visual range, human eye-based visual range, and meteorological optical range. *Atmos. Environ. 190*, 74–86. https://doi.org/10.1016/j.atmosenv.2018.07.020

Kolláth, K. and *Kolláth, Z.*, 2020: On the feasibility of using ceilometer backscatter profile as input data for skyglow simulation. *J. Quantitativ. Spectros. Radiative Trans. 253*, 107158. https://doi.org/10.1016/j.jqsrt.2020.107158

Larson, S.M. and *Cass, G.R.*, 1989: Characteristics of summer midday low-visibility events in the Los Angeles area. *Environ. Sci. amp; Technol.23*, 281–289. https://doi.org/10.1021/es00180a003

Li, S., Joseph, E., Min, Q., Yin, B., Sakai, R., Payne, M.K., 2017: Remote sensing of PM2.5 during cloudy and nighttime periods using ceilometer backscatter. *Atmosp. Measur. Techn. 10*, 2093–2104. https://doi.org/10.5194/amt-10-2093-2017

Molnar, A., Meszaros, E., Imre, K., and *Rull, A.*, 2008: Trends in visibility over Hungary between 1996 and 2002. *Atmos. Environ. 42*, 2621–2629. https://doi.org/10.1016/j.atmosenv.2007.05.012

Münkel, C., Eresmaa, N., Räsänen, J., and *Karppinen, A.*, 2006: Retrieval of mixing height and dust concentration with lidar ceilometer. *Bound.-Lay. Meteorol. 124*, 117–128. https://doi.org/10.1007/s10546-006-9103-3

Muñoz, R.C. and *Alcafuz, R.I.*, 2012: Variability of urban aerosols over Santiago, Chile: Comparison of surface PM10 concentrations and remote sensing with ceilometer and lidar. *Aerosol Air Qual. Res. 12*, 8–19. https://doi.org/10.4209/aaqr.2011.08.0133

Nowak, D., Ruffieux, D., Agnew, J.L., and *Vuilleumier, L.*, 2008: Detection of fog and low cloud boundaries with ground-based remote sensing systems. *J. Atmos. Ocean.Technol. 25*, 1357–1368. https://doi.org/10.1175/2007jtecha950.1

Shepard, F.D., 1996: Reduced visibility due to fog on the highway. Transportation Research Board.

Taillade, F., Belin, E., and *Dumont, E.*, 2008: An analytical model for backscattered luminance in fog: Comparisons with Monte Carlo computations and experimental results. *Measur. Sci. Technol. 19*, 055302. https://doi.org/10.1088/0957-0233/19/5/055302

Wang, J., Liu, X., Yang, X., Lei, M., Ruan, S., Nie, K., Miao, Y., and *Liu, J.*, 2014: Development and evaluation of a new digital photography visiometer system for automated visibility observation. *Atmos. Environ. 87*, 19–25. https://doi.org/10.1016/j.atmosenv.2013.12.045

Wang, R., Gong, J., Wang, Y., Chen, H., Chen, S., and *Wang, Q.*, 2017: Relationship between gross domestic product and accident in china. *J. Safety Stud. 3*, 19. https://doi.org/10.5296/jss.v3i1.10571

Wang, X., Chen, J., Cheng, T., Zhang, R., and *Wang, Xinming*, 2014: Particle number concentration, size distribution and chemical composition during haze and photochemical smog episodes in Shanghai. *J. Environ. Sci. 26*, 1894–1902. https://doi.org/10.1016/j.jes.2014.07.003

Werner, C., Streicher, J., Leike, I., and *Münkel, C.*, 2006: Visibility and Cloud Lidar, In: Lidar: Range-Resolved Optical Remote Sensing of the Atmosphere. Springer Science & Business, 165–186.

Zhao, H., Che, H., Zhang, X., Ma, Y., Wang, Yangfeng, Wang, H., and *Wang, Yaqiang*, 2013: Characteristics of visibility and particulate matter (PM) in an urban area of Northeast China. *Atmos. Pollut. Res. 4*, 427–434. https://doi.org/10.5094/apr.2013.049